Published OnlineFirst May 5, 2008; DOI: 10.1158/1541-7786.MCR-07-2001

BRAF Silencing by Short Hairpin RNA or Chemical Blockade by PLX4032 Leads to Different Responses in Melanoma and Thyroid Carcinoma Cells

Elisa Sala,[1] Luca Mologni,[1] Silvia Truffa,[2] Carlo Gaetano,[2] Gideon E. Bollag,[3] and Carlo Gambacorti-Passerini[1,4]

[1]University of Milano-Bicocca, Monza, Italy; [2]Istituto Dermopatico dell'Immacolata, Rome, Italy; [3]Plexxikon, Inc., Berkeley, California; and [4]McGill University, Montreal, Quebec, Canada

Abstract

BRAF-activating mutations have been reported in several types of cancer, including melanoma (~70% of cases), thyroid (30-70%), ovarian (15-30%), and colorectal cancer (5-20%). Mutant BRAF has constitutive kinase activity and causes hyperactivation of the mitogen-activated protein kinase pathway. BRAF silencing induces regression of melanoma xenografts, indicating the essential role of BRAF for cell survival. We set up an inducible short hairpin RNA system to compare the role of oncogenic BRAF in thyroid carcinoma versus melanoma cells. Although BRAF knockdown led to apoptosis in the melanoma cell line A375, the anaplastic thyroid carcinoma cell ARO underwent growth arrest upon silencing, with little or no cell death. Reexpression of the thyroid differentiation marker, sodium iodide symporter, was induced after long-term silencing. The different outcome of BRAF down-regulation in the two cell lines was associated with an opposite regulation of $p21^{CIP1/WAF1}$ expression levels in response to the block of the BRAF mitogenic signal. These results were confirmed using a specific BRAF small-molecule inhibitor, PLX4032. Restoration of $p21^{CIP1/WAF1}$ expression rescued melanoma cells from death. Altogether, our data indicate that oncogenic BRAF inhibition can have a different effect on cell fate depending on the cellular type. Furthermore, we suggest that a BRAF-independent mechanism of cell survival exists in anaplastic thyroid cancer cells. (Mol Cancer Res 2008;6(5):751–9)

Introduction

The mitogen-activated protein kinase (MAPK) cascade is physiologically activated by binding of a ligand to its membrane-bound receptor tyrosine kinase. Autophosphorylation of specific residues in the intracellular portion of the receptor enables the recognition of downstream effectors, such as Shc, that mediate the recruitment of Grb2-SOS complexes, thus stimulating guanine nucleotide exchange and activation of RAS. GTP-bound RAS, in turn, promotes the activation of RAF family proteins (ARAF, BRAF, CRAF) and then, through MEK1/2 and ERK1/2, the signal reaches the nucleus and a cellular response to the initial stimulus is delivered. This pathway is constitutively activated in numerous human cancers through mutations in a receptor, or in downstream RAS or RAF proteins. Large-scale genomic screens have identified mutations in the *BRAF* gene in several cancers, such as malignant melanoma, colorectal cancer, and ovarian cancer (1). Recently, activating mutations of *BRAF* have also been reported in papillary thyroid carcinoma (PTC; refs. 2-4). The most frequent alteration in the *BRAF* gene, accounting for ~90% of cases, is a T1799A transversion in codon 15 that translates into a V600E amino acid substitution. The presence of negatively charged glutamate in mutant BRAF destabilizes the regulatory interaction between the activation loop and the glycine-rich phosphate-binding loop in the kinase domain, resulting in hyperactivation of BRAF and hence of the MAPK pathway (5). A high proportion of common nevi and the majority of melanomas from sun-exposed sites show BRAF alterations (6, 7) and mutations persist from the primary lesion through later stages of the vertical growth phase and to metastatic disease. In PTCs, BRAF deregulation seems to occur early in tumor development, as indicated by the evidence of BRAF abnormalities in microscopic and preneoplastic lesions (2). Again, BRAF mutations have been identified in all stages of tumor progression, including poorly differentiated and anaplastic carcinomas (8). Anaplastic thyroid carcinoma (ATC) is one of the most aggressive forms of cancer, with a median life expectancy of <1 year at diagnosis, and is believed to arise from dedifferentiation of papillary and follicular carcinomas. An alternative mechanism of BRAF hyperactivation in PTC involves a chromosomal paracentric inversion that leads to the expression of the AKAP9-BRAF fusion protein. As a result of the chromosomal rearrangement, BRAF loses the regulatory conserved regions at the NH_2 terminus and shows 6-fold higher activity compared with wild-type protein (9).

In melanoma cells, $BRAF^{V600E}$ causes deregulated proliferation by overcoming the G_1 restriction point (10) and causing cyclin D1 production in mid-G_1 (11). Karasarides and coworkers showed that both proliferative and survival stimuli were lacking upon depletion of BRAF by small interfering RNA (12). Furthermore, BRAF silencing induces the regression of

Received 8/23/07; revised 12/14/07; accepted 1/22/08.
The costs of publication of this article were defrayed in part by the payment of page charges. This article must therefore be hereby marked *advertisement* in accordance with 18 U.S.C. Section 1734 solely to indicate this fact.
Requests for reprints: Luca Mologni, University of Milano-Bicocca, via Cadore 48, Monza, 20052 Italy. Phone: 39-2644-88059; Fax: 39-2644-88363. E-mail: luca.mologni@unimib.it

doi:10.1158/1541-7786.MCR-07-2001

Published OnlineFirst May 5, 2008; DOI: 10.1158/1541-7786.MCR-07-2001

human melanoma xenografts (13). The role of BRAF signaling in thyroid tumorigenesis has been studied in PCCL3 rat thyroid cell lines. Mitsutake et al. (14) showed that conditional $BRAF^{V600E}$ expression decreases dependence from thyrotropin for growth and impairs the synthesis of thyroid markers such as sodium iodide symporter (NIS), thyroglobulin, and Pax8. In line with these data, BRAF mutation is frequently associated with loss of ^{131}I avidity and treatment failure in PTC (15).

In this work, we compared the *in vitro* responses of melanoma and thyroid carcinoma cell lines to BRAF inhibition obtained pharmacologically and by short hairpin RNA (shRNA), in order to understand the mechanisms by which the same oncogene induces tumorigenesis in different cell types.

Results

BRAF Validation

We used A375 and ARO cell lines as models for melanoma and thyroid carcinoma, respectively, and generated clones expressing an inducible shRNA targeting BRAF under the control of doxycycline. A shRNA sequence that had been validated in previous studies was chosen (12, 13, 16). Silencing of BRAF protein, and the consequent down-regulation of phosphorylated MEK1/2 levels, were evaluated by Western blot after 72 and 96 hours of treatment with doxycycline. Densitometric analysis of bands from induced and noninduced samples indicated that BRAF was down-regulated by >70% in both cell lines after 96 hours of doxycycline treatment (Fig. 1). Concomitant down-regulation of MEK1/2 phosphorylation was also observed.

As a consequence of BRAF modulation, cell growth was significantly delayed in ARO cells and completely arrested in A375 melanoma cell line (Fig. 2A-B). Cells that were transfected only with the regulatory plasmid were not affected by doxycycline (data not shown). Viable cell counts using trypan blue dye revealed substantial cell death in A375 but not in the ARO population (data not shown). Cell cycle analysis showed a significant induction of apoptosis in the A375 cell line (visualized as an increased sub-G_1 fraction) with a concurrent decrease in the G_1 population and an increase of the G_2-M peak (Fig. 2C). By contrast, in ARO cells, only a small increase of the G_1 peak was noted accompanied by a significant decrease of the G_2-M fraction (Fig. 2D). In order to confirm these data, Annexin V staining was carried out after vehicle or doxycycline treatment (Fig. 2E-F). Although no or very few Annexin V–positive cells were found in the ARO population, ~25% of A375 cells underwent apoptosis after 96 hours of exposure to doxycycline, in line with cell cycle data.

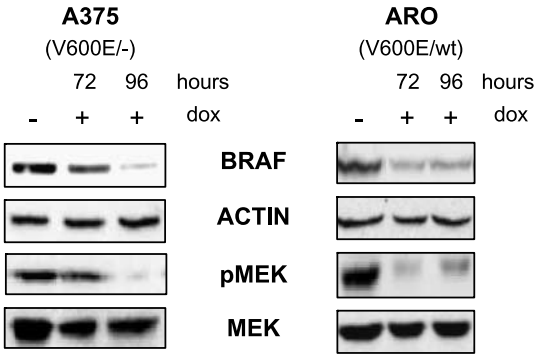

FIGURE 1. Down-regulation of BRAF protein by shRNA. Melanoma (*A375*) and ATC (*ARO*) cells were left untreated (–) or treated with 1 μg/mL of doxycycline (+) for 72 or 96 h. Cell lysates were loaded on polyacrylamide gels and analyzed with the indicated antibodies. MEK1/2 phosphorylation status is reported (*pMEK*) as a marker of MAPK pathway activation. Antiactin and total MEK1/2 immunoblottings were used as loading controls.

In the absence of cell death, a possible explanation for ARO growth delay could be the induction of differentiation. Thus, using Western blotting, we analyzed the expression levels of NIS after 8 days of continuous BRAF silencing. NIS is responsible for the uptake of iodine in normal thyrocytes and radioactive iodine-131 in targeted therapies against differentiated thyroid cancer. Reexpression of NIS, if correctly located at the cell membrane, would also allow ^{131}I therapy in tumors that had lost this function. As shown in Fig. 2G, NIS was reexpressed in correspondence with complete BRAF silencing. In summary, BRAF depletion induces apoptosis in melanoma cells and differentiation but not apoptosis in ATC cells.

PLX4032 Characterization

Having validated BRAF as a possible therapeutic target, we proceeded to the biochemical characterization of a new BRAF inhibitor, PLX4032, in order to confirm the shRNA results with a pharmacologic approach that is more applicable from a clinical standpoint. PLX4032 is a highly selective inhibitor of BRAF kinase activity, with an IC_{50} of 44 nmol/L against V600E-mutant BRAF. From a panel of 65 non-RAF kinases covering much of the kinome, only one kinase—BRK (also known as PTK6)—showed inhibition in the nanomolar range (IC_{50} = 240 nmol/L). Most of the kinases tested showed >100-fold higher IC_{50} (data not shown). PLX4032 is currently undergoing clinical evaluation (17). We tested this compound on the melanoma cell line A375 and on three thyroid carcinoma cell lines (ARO, NPA, and TPC-1). Dose-response curves obtained using a proliferation read-out indicated an efficient antiproliferative activity of PLX4032 in all BRAF-dependent cellular systems at nanomolar doses (Fig. 3A; Table 1). The compound was most potent in A375 cells (IC_{50} = 47 nmol/L). Thyroid cancer ARO and NPA cells were less sensitive and showed similar inhibition (IC_{50} = 205 nmol/L and IC_{50} = 126 nmol/L, respectively). TPC1 showed an approximately 50-fold higher IC_{50} value (IC_{50} = 10.77 μmol/L), likely due to the presence of alternative signaling pathways activated by RET/PTC1. Western blot analysis confirmed the block of BRAF-mediated MEK1/2 phosphorylation in a dose-dependent manner in A375, NPA, and ARO cells (Fig. 3B). In line with the proliferation data, MEK1/2 phosphorylation was not affected by PLX4032 in TPC1 cells.

PLX4032 promoted apoptotic death in A375 cells in a dose-dependent manner, as assessed by Annexin V–staining (Fig. 4A), by the appearance of a subdiploid peak in cell cycle analysis (Fig. 4B) and by activation of caspase-3 (Fig. 4C). These results confirm that BRAF provides a survival signal in

Published OnlineFirst May 5, 2008; DOI: 10.1158/1541-7786.MCR-07-2001

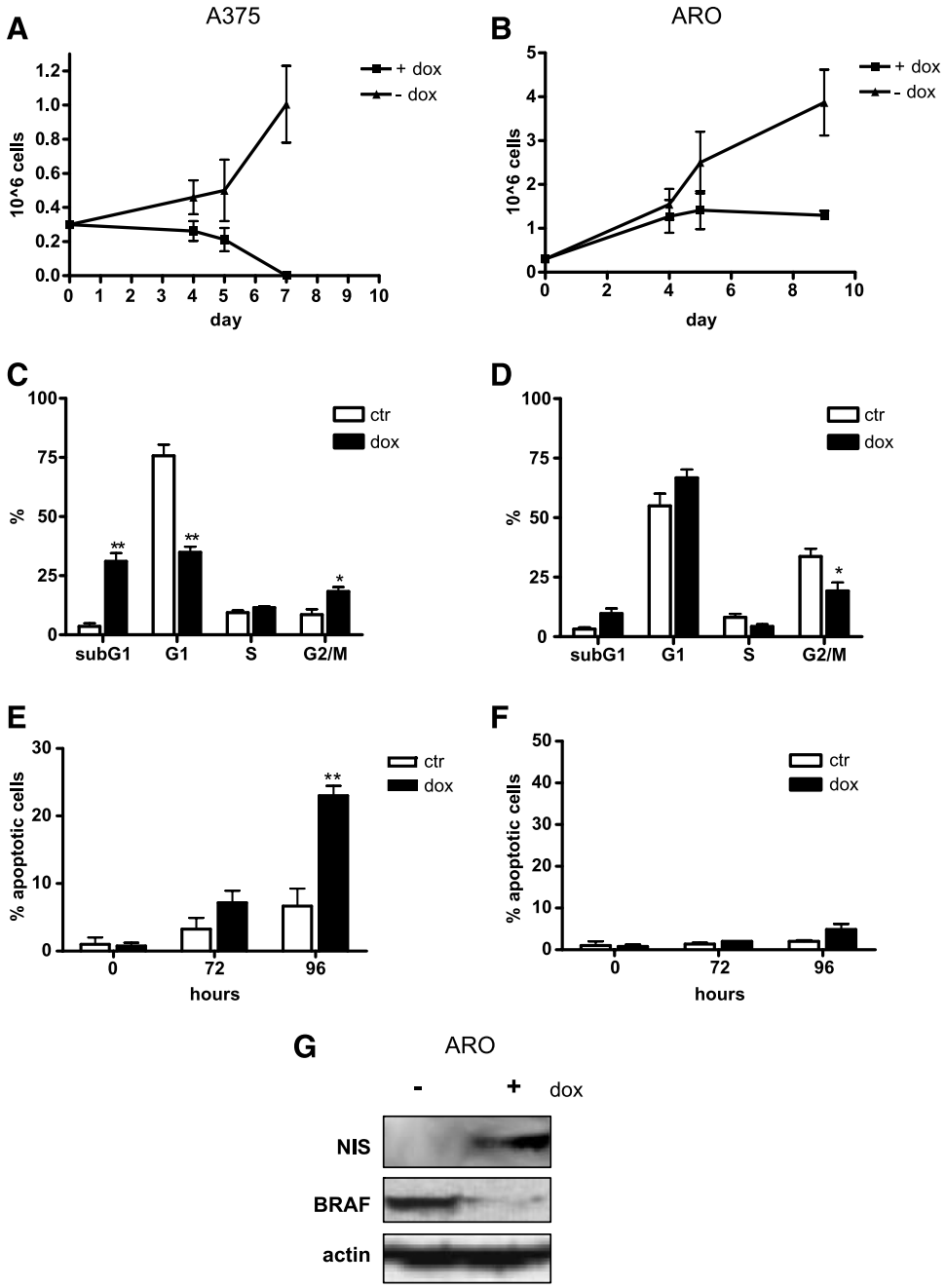

FIGURE 2. Biological effects of BRAF silencing: growth curves of A375 (**A**) and ARO (**B**) cell lines in the absence or presence of doxycycline. Cells were counted by trypan blue exclusion assay. **C** and **D.** Cell cycle analysis of A375 (**C**) and ARO (**D**) cells after 96 h of shRNA induction. An increase in sub-G_1 fraction is evident in A375 cells, whereas the ARO cell line showed a decrease of the G_2-M peak. **E** and **F.** Annexin V staining of A375 (**E**) and ARO (**F**) cells was assayed before (time 0) and 48 to 96 h after vehicle or doxycycline treatment. White columns, control cells; black columns, doxycycline-treated cells; the average of triplicate samples is always reported, with SD (*, $P < 0.01$; **, $P < 0.001$). **G.** ARO cells were treated with vehicle alone (−) or doxycycline (+) for 9 d; induction of NIS expression is shown by Western blot. Actin was used as a loading control.

this melanoma cell line. By contrast, in thyroid cancer cell lines NPA and ARO, very little evidence of apoptosis was observed in several experiments (Fig. 4D-I). An arrest in G_1 and a decrease of S and G_2-M phases were observed in these cells, in accordance with results obtained by shRNA (data not shown). In TPC1 cells, neither apoptosis nor cell cycle alterations were observed at up to 10 μmol/L of PLX4032 (data not shown). These results on thyroid cell lines are consistent with recently published BRAF inhibitor data (18). In ARO cells, long-term treatment (6 days) with PLX4032 induced the reexpression of the NIS pump (Fig. 5B), again confirming shRNA data.

From these results, we can conclude that the pharmacologic inhibition of BRAF enzymatic activity has the same consequences as down-regulation of its expression, in terms of cell growth and alterations of the cell cycle. These data also indicate that PLX4032 is specifically active on BRAF-mutated cell lines.

Differential Molecular Effects of BRAF Inhibition in Melanoma versus Thyroid Carcinoma Cells

We then hypothesized an involvement of other cell signaling pathways and looked for changes in the expression of antiapoptotic factors or cell cycle regulators. We used shRNA to make sure that the effects were specifically related to BRAF

Published OnlineFirst May 5, 2008; DOI: 10.1158/1541-7786.MCR-07-2001

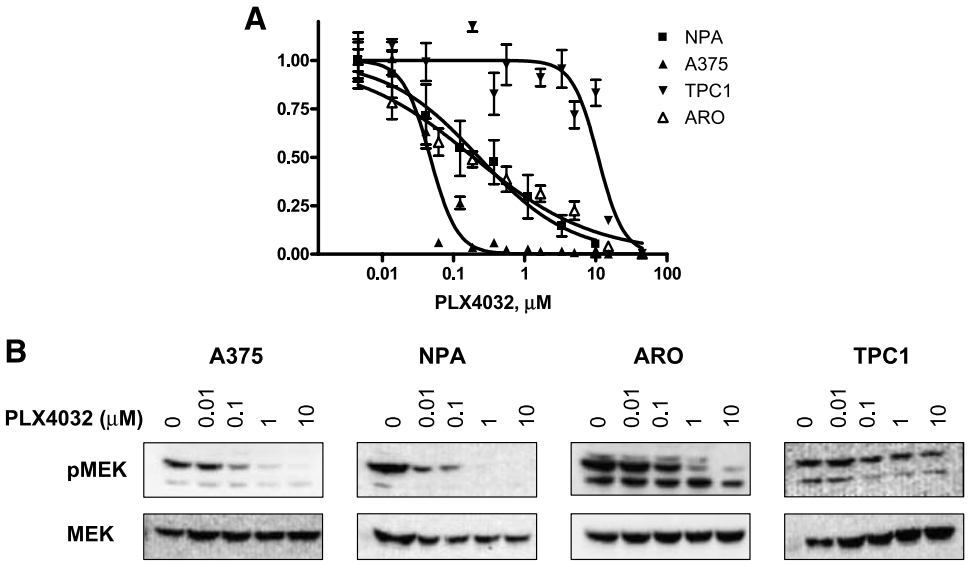

FIGURE 3. BRAF inhibition by PLX4032. **A.** Relative proliferation assessed by the ^{3}H-thymidine incorporation assay of the indicated cell lines in the presence of increasing concentrations of PLX4032. **B.** Effects of BRAF inhibition on the phosphorylation of its direct substrate, MEK1/2. Cells treated for 4 h with the indicated doses of PLX4032 were lysed and probed with anti-phosphorylated MEK1/2 and anti-MEK1/2 antibodies.

silencing. The results were then confirmed by treatment with PLX4032 to ensure that they were not due to unspecific effects of doxycycline or off-target effects of the shRNA. As reported in Fig. 5, increased phosphorylation of AKT (Ser^{473}) was observed in both cell lines when the BRAF/MAPK pathway was switched off. No changes were seen in the expression levels of the antiapoptotic factors BCL2 (data not shown) or BCL_{XL}. By contrast, we noted an intriguing difference in $p21^{CIP1/WAF1}$ expression: A375 cells down-regulated $p21^{CIP1/WAF1}$ in response to BRAF silencing, whereas ARO up-regulated it. Levels of $p27^{Kip1}$ were slightly decreased in A375 cells whereas they remained unaltered in ARO.

An important difference between A375 on one hand, and ARO and NPA on the other, lies in their p53 status: A375 express the wild-type protein whereas ARO and NPA have mutated, inactive p53. Therefore, we considered the possibility that p53 plays a major role in the sensitivity to apoptosis in BRAF-silenced cells. ARO cells expressing a temperature-sensitive p53 protein, which has wild-type activity at 32°C and is inactive at 37°C (19), were treated with 10 μmol/L of PLX4032 and either kept at 37°C or shifted to the permissive temperature. No evidence of apoptosis was observed (results not shown). On the other hand, the SK-Mel28 melanoma cell line, expressing mutated p53, showed a sensitivity to PLX4032 comparable to A375 (data not shown). These results suggested that the effects of BRAF inhibition in thyroid carcinoma and melanoma cell lines are independent of p53 activity.

Table 1. IC_{50} Values with 95% Confidence Intervals for Each Cell Line (Mean Of Three Independent Experiments)

	IC_{50} (μmol/L)	95% Confidence intervals
A375	0.0472	0.0406-0.0545
NPA	0.1260	0.0735-0.2159
ARO	0.2051	0.1295-0.3250
TPCI	10.77	8.34-13.91

Effects of $p21^{CIP1/WAF1}$ Modulation

Expression of $p21^{CIP1/WAF1}$ was regulated in opposite directions in melanoma and thyroid cells. Therefore, we reasoned that $p21^{CIP1/WAF1}$ might be the molecular switch that determines the outcome of BRAF inhibition. To evaluate the role of $p21^{CIP1/WAF1}$ in the resistance to apoptosis, two adenoviral constructs were employed: one that encodes for $p21^{CIP1/WAF1}$ (Ad.p21-S) to restore $p21^{CIP1/WAF1}$ levels in A375, whereas the second one (Ad.p21-AS) encodes for an antisense transcript and was exploited to knock down $p21^{CIP1/WAF1}$ protein in ARO cells (20). Cells were simultaneously infected by the adenovirus and treated with PLX4032. We used PLX4032 to obtain an immediate block of BRAF activity and consequent change in $p21^{CIP1/WAF1}$ levels. Effects on the cell cycle were evaluated by propidium iodide staining. As shown in Fig. 6A, PLX4032 caused dose-dependent apoptosis in A375 cells, as expected. However, concomitant overexpression of $p21^{CIP1/WAF1}$ induced by the sense adenoviral construct (Fig. 6A, *bottom*), protected A375 cells from PLX4032-induced programmed cell death. On the other hand, down-regulation of endogenous $p21^{CIP1/WAF1}$ in ARO cells (Fig. 6B) reversed PLX4032-mediated effects on the cell cycle: the G_2-M fraction was increased to the same level of untreated cells. However, no apoptosis was observed in ARO cells after $p21^{CIP1/WAF1}$ knock-down (data not shown). No effect was induced by infection with control green fluorescent protein (GFP)–only adenovirus (data not shown). Viability was also determined by trypan blue exclusion assay and caspase-3 activity assay (data not shown), confirming cell cycle data. Annexin V staining could not be measured because of interference in the green channel by viral expression of GFP (see Materials and Methods).

Altogether, our data suggest an involvement of $p21^{CIP1/WAF1}$ in cell cycle arrest, but not in apoptosis, in the ARO cell line, whereas in A375 cells, the down-regulation of $p21^{CIP1/WAF1}$ seems to be relevant for the induction of programmed cell death.

Published OnlineFirst May 5, 2008; DOI: 10.1158/1541-7786.MCR-07-2001

Discussion

Targeted therapies offer the potential to selectively kill tumors while sparing normal tissues. The assumption behind this strategy is that tumors are tightly dependent on the continuous activity of an oncogene. This concept is best proven by chronic myeloid leukemia, in which imatinib therapy induces regressions in almost all cases including advanced disease (21). Most importantly, Bcr-Abl activity is restored in imatinib-resistant cells by point mutations that make the target kinase refractory to inhibition. Although chronic myeloid leukemia is a perfect case for molecular targeting, most tumors show several genetic aberrations that are acquired throughout their development. Identifying the founder events, to which the tumor may be "addicted", is instrumental to the development of new targeted therapies. Although the most desirable effect of oncogene turn-off would be the death of tumor cells, induction of terminal differentiation is an excellent therapeutic alternative, as differentiated cells only have a limited life span. For example, disruption of β-catenin activity in colon cancer cells induces $p21^{CIP1/WAF1}$ expression, G_1 arrest, and differentiation with no apoptosis (22).

BRAF is the most common lesion in PTC and this alteration does not overlap with RET/PTC translocations, indicating that they both impinge on the same pathway. We set up an inducible shRNA to silence BRAF expression in the ARO and A375 cell lines under control of doxycycline (23). A375 was recently used to validate BRAF as a therapeutic target in melanoma (13). Stably transfected cell lines allow long-term experiments without losing silencing efficiency. shRNA efficiently worked in both cell lines, suppressing BRAF expression within 96 hours and down-regulating MAPK signaling. BRAF down-regulation induced apoptosis in melanoma cells and growth delay but not apoptosis in ATC cells. Restoration of NIS expression was achieved in ARO. NIS is responsible for iodine uptake in thyroid cells when correctly located at the cell

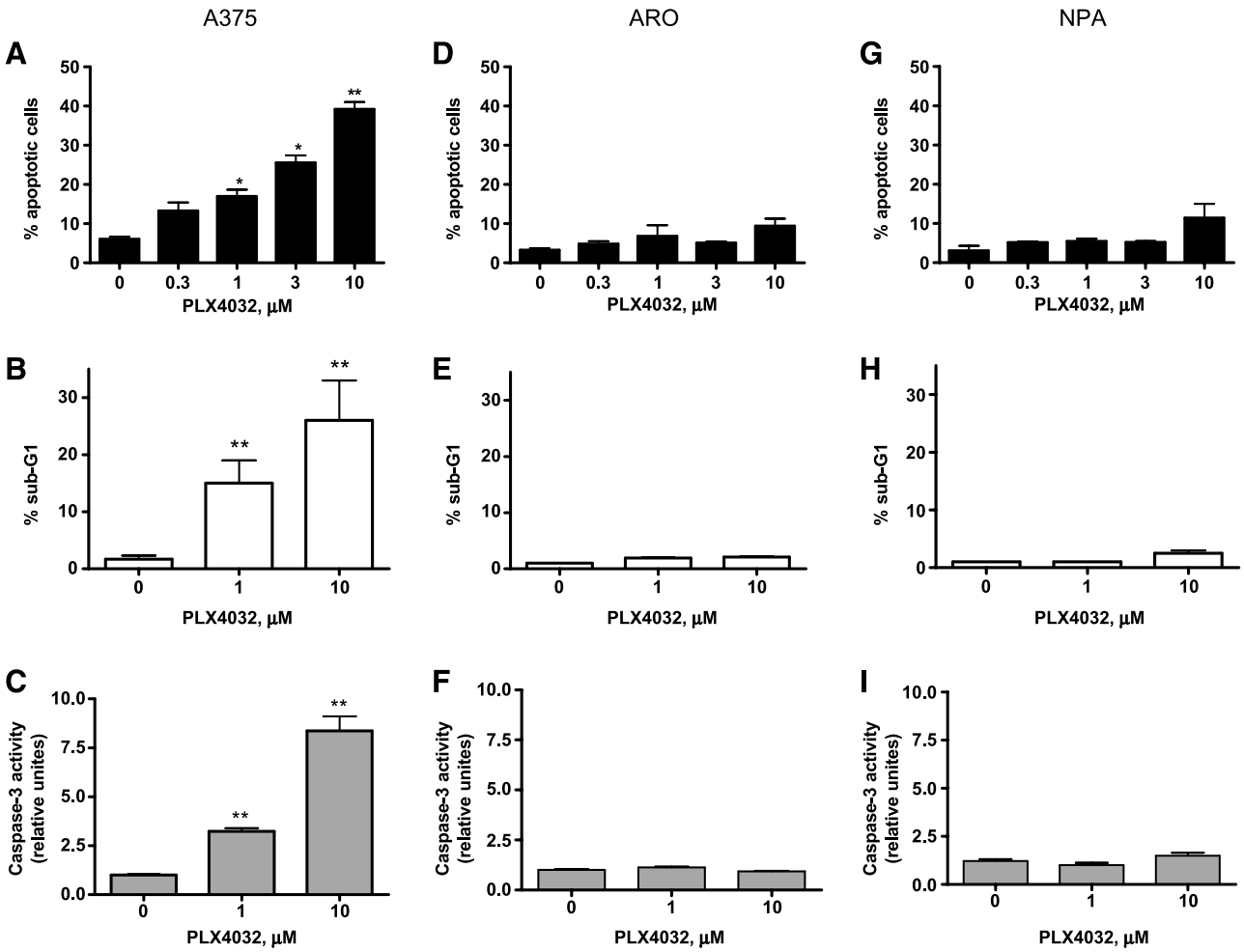

FIGURE 4. Effects of PLX4032 on cell death. A375 (**A-C**), ARO (**D-F**), and NPA (**G-I**) cells were treated with increasing doses of PLX4032 and the percentage of apoptotic cells was determined by Annexin V binding assay (**A, D,** and **G**), propidium iodide quantification of the sub-G_1 population (**B, E,** and **H**), or caspase-3 enzymatic assay (**C, F,** and **I**; *, $P < 0.01$; **, $P < 0.001$). Columns, mean of three replicates; bars, SD. The graphs are representative of four independent experiments.

Published OnlineFirst May 5, 2008; DOI: 10.1158/1541-7786.MCR-07-2001

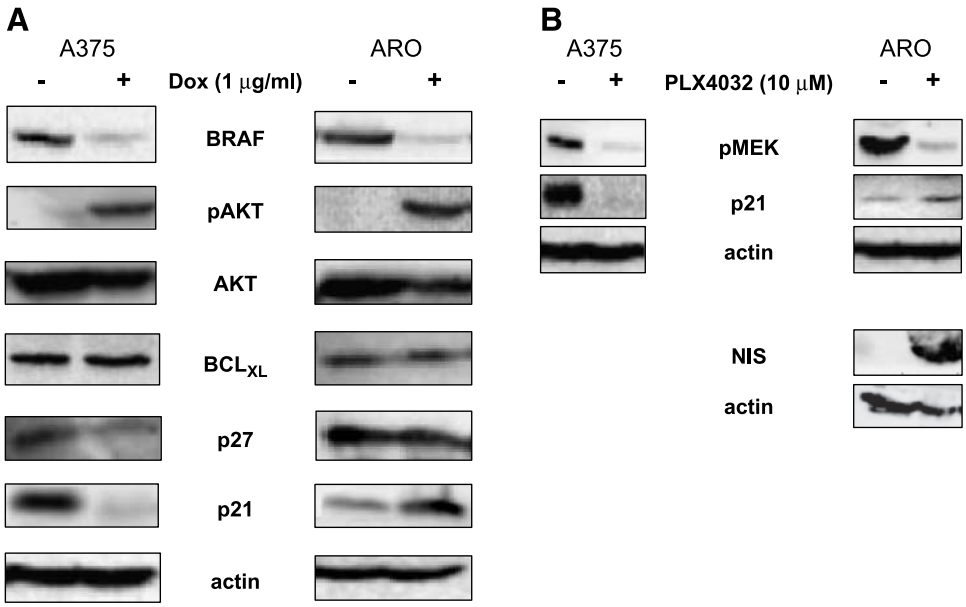

FIGURE 5. Molecular effects of BRAF silencing (**A**) or pharmacologic inhibition (**B**) in melanoma and thyroid carcinoma cell lines. **A.** Cells were grown in the absence (−) or presence (+) of doxycycline for 96 h. Total lysates were immunoblotted with the indicated antibodies. **B.** Cells treated with 10 μmol/L of PLX4032 for 72 h (*top*) or 6 d (*bottom*) were lysed and probed with the indicated antibodies.

membrane. Reexpression of NIS is a clear marker of thyroid cell differentiation. Recent studies showed that $BRAF^{V600E}$ expression induces dedifferentiation of PCCL3 rat thyroid cells with significant loss of NIS at the cell membrane and decrease of its expression within 6 days (14). Our data showed NIS reexpression with the same timing in ARO, confirming that BRAF plays an important role in this process. Given the favorable prognosis of differentiated thyroid carcinoma as compared with ATC, induction of redifferentiation might be the first step to control tumor growth as well as being an attractive tool for the clinical management of ATC.

A novel BRAF small-molecule inhibitor was characterized in one melanoma cell line (A375) and three PTC cell lines (ARO, NPA, and TPC1). Differences in the genetic background of these cells allows for the evaluation of the response in a wider model. PLX4032 showed nanomolar activity against all cell lines that carry BRAF mutation and at least 50-fold higher IC_{50} against BRAF wild-type TPC1 cells. This significant difference can be related to the multiplicity of signaling pathways activated by RET/PTC oncogenes. It is interesting to note that the IC_{50} obtained with ARO cells (205 nmol/L) is slightly but reproducibly higher than that seen with NPA (126 nmol/L). This result correlates with the respective BRAF mutational status because PLX4032 is more potent against $BRAF^{V600E}$ than the wild-type protein,[5] whereas ARO are heterozygous for the mutation, and no wild-type allele is present in NPA.

A decrease in MEK1/2 phosphorylation indicated that BRAF was effectively blocked by PLX4032: the doses needed to block MEK1/2 phosphorylation were consistent with the IC_{50} values. The RAF-MEK1/2-ERK1/2 cascade regulates the progression through G_1 to S phase in melanoma (24), whereas in thyroid cancer, recent evidences point to an involvement of the MAPK pathway in the G_2-M checkpoint (25). Therefore, we analyzed the cell cycle and viability of PLX4032-treated cells: A375 showed high levels of apoptosis, as expected from the results obtained with inducible shRNA, whereas thyroid cancer cell lines showed only G_1 arrest, decrease in G_2-M phase, and a little apoptosis at the highest dose. Similarly, in recent works (18, 26), BRAF inhibition impaired the progression of thyroid carcinoma cells into S and G_2-M phase and caused G_1 arrest, without inducing apoptosis, at least at short exposure times. In contrast with the data reported by Ouyang et al. (18), TPC1 were not affected by the inhibition of BRAF. This discrepancy may be related to the selectivity of the compounds used. Indeed, as Ouyang et al. state in their article, LBT613 blocks RET kinase activity *in vitro*. For this and other reasons, concerns about the specificity of BRAF molecules have been raised (27).

We excluded that the cellular response to BRAF inhibition was dependent on p53. Then, we tried to explain the different behaviors between melanoma and thyroid carcinoma cell lines. Activation of AKT was seen in both cell types following shRNA induction and was not due to doxycycline per se, as this effect was not observed in parental cells. Activation of the AKT survival pathway may be a reaction to MAPK signal suppression. However, treatment of ARO cells with the phosphoinositide-3-kinase inhibitor, LY294002, had no effect on cell survival (data not shown).

In contrast, $p21^{CIP1/WAF1}$ was differentially regulated in melanoma and thyroid carcinoma cell lines, and this correlated with the outcome of BRAF signaling inhibition. Overexpression of $p21^{CIP1/WAF1}$ largely saved melanoma A375 cells from PLX4032-induced cell death. Up-regulation of $p21^{CIP1/WAF1}$ has been implicated in the resistance to stress-induced apoptosis in various cellular systems (28, 29). Melanoma cells that fail to induce $p21^{CIP1/WAF1}$ die upon p53 overexpression (30). These and our data point to the role of $p21^{CIP1/WAF1}$ as a master switch

[5] Unpublished data.

Published OnlineFirst May 5, 2008; DOI: 10.1158/1541-7786.MCR-07-2001

in the decision between growth arrest (with or without consequent differentiation) and apoptosis, at least in melanoma. In ARO cells, down-regulation of $p21^{CIP1/WAF1}$ by antisense RNA did not cause cell death, suggesting that additional factors influence cell survival in ATC. The identification of additional genetic abnormalities which prevent ATC from developing apoptosis will increase the therapeutic potential for this tumor. It should be noted that the data presented here on $p21^{CIP1/WAF1}$ regulation only refer to one melanoma and one ATC cell line, although the results are in line with previous observations.

In conclusion, our data support the view of a crucial role of BRAF in melanoma survival and thyroid cancer dedifferentiation, and the possibility to treat these tumors, especially melanoma, using small-molecule inhibitors. PLX4032 showed high efficacy and specificity against BRAF-mutated cell lines, but not against RET/PTC-positive cell lines. These results provide evidence for the importance of directly targeting oncogenic proteins involved in the malignant transformation process.

Materials and Methods

Cells and Reagents

The A375 malignant melanoma cell line has a mutated $BRAF^{V600E}$ and no wild-type allele (31), and expresses wild-type p53 (32). SK-Mel28 melanoma cells have mutated $BRAF^{V600E}$ and inactive p53. Undifferentiated ATC cells (ARO) are heterozygous for *BRAF* mutation (V600E/wt) and carry an inactivating mutation on one *TP53* allele (33). NPA, derived from a poorly differentiated thyroid carcinoma, carry only the $BRAF^{V600E}$ allele and have mutated p53 (2). TPC1, established from a well-differentiated PTC, harbors the RET-PTC1 translocation and wild-type *BRAF* (34). All cell lines were grown in DMEM (Bio Whittaker), except for A375, which was maintained in RPMI 1640 (Bio Whittaker). All media were supplemented with 10% fetal bovine serum (of South American origin; Bio Whittaker), 2 mmol/L of L-glutamine, 100 units/mL of penicillin-streptomycin (Sigma-Aldrich), and 100 units/mL of gentamicin. PLX4032 was kindly provided by Plexxikon, Inc. The compound was dissolved in DMSO at 100 mmol/L and stored in small aliquots at −20°C. Due to the serum protein binding properties of PLX4032, it was always used in cell culture medium supplemented with low serum concentrations (typically 5%).

Inducible shRNA System

To generate the anti-BRAF shRNA construct, the following oligonucleotides were used (bases shown in uppercase correspond to the target sequence in BRAF mRNA; ref. 16): BRAF-shRNA-sense, 5′-gatcccAGAATTGGATCTGGATCATttcaagagaATGATCCAGATCCAATTCTttttggaaa-3′. BRAF-shRNA-antisense, 5′-agcttttccaaaaaAGAATTGGATCTGGATCATctcttgaaATGATCCAGATCCAATTCTgg-3′. This sequence was cloned into *Bgl*II and *Hin*dIII sites of pTER vector described by van de Wetering et al. (23). A375 and ARO cells were first transfected with pcDNA6/TR regulatory plasmid (Invitrogen), which encodes the Tet repressor (TetR) under the control of the human cytomegalovirus promoter. TetR binds the Tet operator (TetO) in pTER vector, thereby repressing gene transcription. In the presence of doxycycline, TetR leaves the TetO sites, thus allowing shRNA expression. Stably transfected cells were selected with 4 μg/mL of blasticidin (Sigma-Aldrich). Clones were isolated by limiting dilutions and approximately 30 clones were tested for

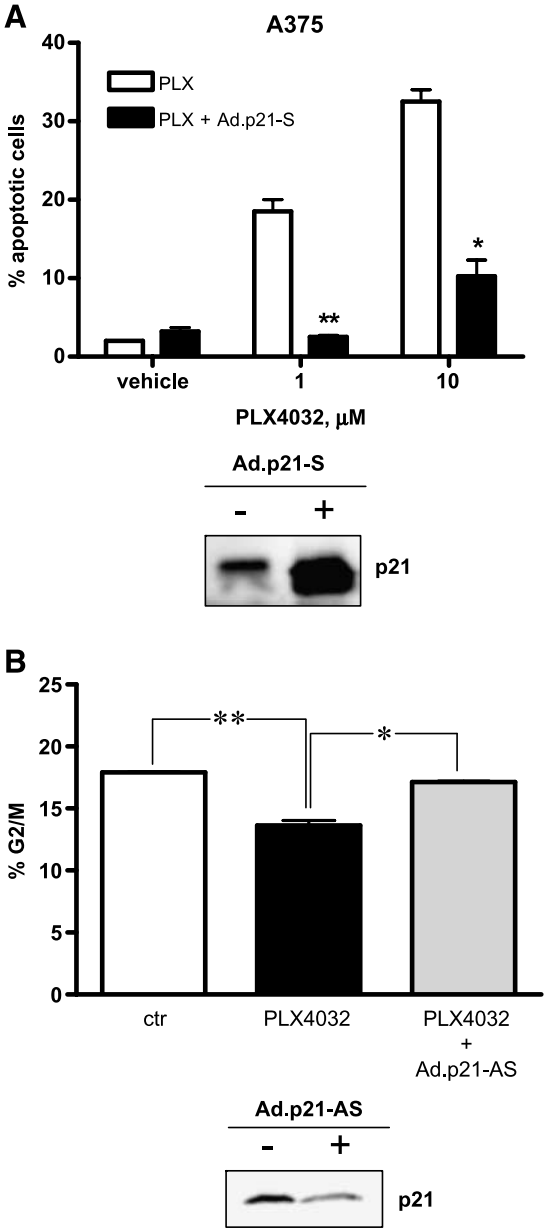

FIGURE 6. Modulation of $p21^{CIP1/WAF1}$ expression by adenoviral infection. **A.** A375 cells were infected with recombinant adenovirus expressing sense $p21^{CIP1/WAF1}$ mRNA (*Ad.p21-S*) and treated with vehicle alone, 1 or 10 μmol/L of PLX4032 for 72 h. The sub-G_1/apoptotic fraction was measured by propidium iodide staining. White columns, noninfected cells; black columns, Ad.p21-S–infected cells. **B.** ARO cells were infected with adenovirus expressing antisense $p21^{CIP1/WAF1}$ transcript (*Ad.p21-AS*) and treated with 1 μmol/L of PLX4032 for 72 h (*gray column*). Noninfected cells were treated with vehicle (*ctr, white column*) or with PLX4032 (*black column*) for 72 h. The percentage of the G_2-M population was determined by propidium iodide staining (*, $P < 0.01$; **, $P < 0.001$). $p21^{CIP1/WAF1}$ expression was assessed by Western blot before and after adenovirus infection, in the presence of PLX4032 (*bottom panels*).

Published OnlineFirst May 5, 2008; DOI: 10.1158/1541-7786.MCR-07-2001

doxycycline-regulated gene expression by transient transfection of the pcDNA4/TO-Luc plasmid (a kind gift from Dr. Hans Clevers, Hubrecht Laboratory, Utrecht, the Netherlands) and reading induced luciferase activity with the dual-luciferase reporter assay kit (Promega) following the manufacturer's protocol. Clones that showed the highest induction by doxycycline and tight repression in the absence of the drug were transfected with the pTER-BRAF-shRNA response plasmid and selected with 600 μg/mL of zeocin (Invitrogen). Stably double-transfected cell lines were cultured in the appropriate medium, adding blasticidin and zeocin at every second passage. All transfections were done by Ca_2PO_4 method. Briefly, 3×10^5 cells were seeded in 2 mL of medium in six-well plates (60% confluence); on the following day, cells were transfected with 1 μg of DNA and incubated at 37°C for 8 h; the transfection mixture was then removed, the cells washed with PBS, shocked with 70% glycerol for 1 min and finally washed twice with PBS. Selection started 72 h after transfection.

Western Blots

Cells (3×10^5) were seeded in six-well plates and harvested after 72 and 96 h of treatment with 1 μg/mL of doxycycline or with PLX4032 at the indicated doses. Cells were then lysed in Laemmli buffer and boiled. Western blotting was done as described (35). Antibodies were used according to the recommended dilutions. Anti-BRAF antibody (C19) was purchased from Santa Cruz Biotechnology. Antibodies specific for phosphorylated MEK1/2 ($Ser^{217-221}$), total MEK1/2, phosphorylated AKT (Ser^{473}), AKT, and $p27^{Kip1}$ were all from Cell Signaling Technology. Anti-BCL_{XL} antibody (7B2.5) was bought from Upstate Biotechnology. Additional antibodies employed in this study recognized $p21^{CIP1/WAF1}$ (clone EA10, Calbiochem), NIS (clone 2.2, Chemicon), and actin (Sigma-Aldrich).

Proliferation Assays

Serial dilutions of inhibitor were prepared in cell culture medium with 5% fetal bovine serum in 96-well plates. Cells were resuspended in 5% fetal bovine serum medium and added to the plate at a density of 10^4 cells/well. Cell proliferation was measured after 72 h using the tritiated-thymidine incorporation assay as described previously (35). Each data point was done in triplicate.

Cell Cycle Analysis and Apoptosis

Cells were seeded in six-well plates at a density of 2×10^5/well and treated as indicated in figure legends. Cells were harvested at 72 and 96 h after treatment, washed with PBS, and fixed in 70% ethanol at −20°C overnight. The samples were then centrifuged and resuspended in PBS containing 50 μg/mL of propidium iodide (Sigma-Aldrich) and 100 μg/mL of RNase A (Sigma-Aldrich), incubated at 37°C for 30 min and analyzed by FACScan flow cytometer (Becton Dickinson).

Annexin V binding assay was done following the manufacturer's protocol (MedSystem Diagnostics). Briefly, cells were treated with BRAF inhibitor or vehicle for 96 h in six-well plates. Cells were then harvested, washed with PBS, and counted. Approximately 10^5 cells were doubly stained with FITC-Annexin V and propidium iodide and analyzed by FACScan flow cytometer. The cell population staining positive for Annexin V and negative for propidium iodide (bottom right quadrant of the green/red fluorescence dot plot) was considered as early apoptotic. Cells treated with 10 μmol/L of staurosporine (A375 and ARO) or 5 mmol/L of valproic acid (NPA) were used as positive controls.

Caspase-3 Activity Measurement

The cells were seeded in triplicate in 24-well plates and treated as described in the figure legends. After 48 h, the cells were harvested and an aliquot was used to determine cell number, using the CellTiter 96 AQueous One Solution Cell Proliferation Assay (Promega Corporation). Briefly, the MTS tetrazolium reagent was added to the cells and incubated for 2 h at 37°C. Absorbance at 490 nm was read with a 96-well plate reader. Background absorbance (medium only) was subtracted from the sample values. The remaining cells were used to measure cellular caspase-3 activity, using Caspase-glo 3/7 Assay (Promega): 100 μL of Caspase-glo reagent was added to 100 μL of cells in 96-well plates and incubated for 1 h at room temperature. Luminescence was read with a 1450 Microbeta Trilux luminescence counter (Perkin-Elmer). Caspase-3 activity readings were normalized on cell number.

Adenovirus Infection

Adenoviruses expressing $p21^{CIP1/WAF1}$ sense or antisense transcripts and GFP as a marker were prepared as described (20). Experiments were done by seeding 3×10^5 cells in complete medium, in six-well plates. On the following day, medium was removed and the adenovirus (diluted in 1 mL of medium containing 2% fetal bovine serum) added to the cells at a multiplicity of infection of 100. After 2 h at 37°C, the viral suspension was removed and fresh medium with or without PLX4032 was supplied. The cells were harvested at 72 or 96 h postinfection. Infection efficiency was evaluated by measuring fluorescence from GFP by FACScan flow cytometer.

Statistical Analysis

Data were always generated in triplicate and mean ± SD is reported in graphs. Dose-response curves were normalized over the vehicle control and analyzed by nonlinear regression using GraphPad PRISM 4.0 software. IC_{50} values were calculated by global fitting of at least three independent experiments, with 95% confidence interval.

Disclosure of Potential Conflicts of Interest

No potential conflicts of interest were disclosed.

Acknowledgments

We thank Plexxikon, Inc., for providing the inhibitor PLX4032. We are also grateful to Dr. Hans Clevers (Hubrecht Institute, Utrecht, the Netherlands) for the pTER plasmid and to Dr. Michela Viltadi for excellent technical assistance.

References

1. Davies H, Bignell GR, Cox C, et al. Mutations of the BRAF gene in human cancer. Nature 2002;417:949–54.

2. Nikiforova MN, Kimura ET, Gandhi M, et al. BRAF mutations in thyroid

Published OnlineFirst May 5, 2008; DOI: 10.1158/1541-7786.MCR-07-2001

tumors are restricted to papillary carcinomas and anaplastic or poorly differentiated carcinomas arising from papillary carcinomas. J Clin Endocrinol Metab 2003;88:5399–404.

3. Trovisco V, Vieira de Castro I, Soares P, et al. BRAF mutations are associated with some histological types of papillary thyroid carcinoma. J Pathol 2004;202:247–51.

4. Fugazzola L, Puxeddu E, Avenia N, et al. Correlation between B-RAFV600E mutation and clinico-pathologic parameters in papillary thyroid carcinoma: data from a multicentric Italian study and review of the literature. Endocr Relat Cancer 2006;13:455–64.

5. Wan PT, Garnett MJ, Roe SM, et al. Mechanism of activation of the RAF-ERK signaling pathway by oncogenic mutations of B-RAF. Cell 2004;116:855–67.

6. Pollock PM, Harper UL, Hansen KS, et al. High frequency of BRAF mutations in nevi. Nat Genet 2003;33:19–20.

7. Cohen Y, Rosenbaum E, Begum S, et al. Exon 15 BRAF mutations are uncommon in melanomas arising in nonsun-exposed sites. Clin Cancer Res 2004;10:3444–7.

8. Adeniran AJ, Zhu Z, Gandhi M, et al. Correlation between genetic alterations and microscopic features, clinical manifestations, and prognostic characteristics of thyroid papillary carcinomas. Am J Surg Pathol 2006;30:216–22.

9. Ciampi R, Knauf JA, Kerler R, et al. Oncogenic AKAP9-BRAF fusion is a novel mechanism of MAPK pathway activation in thyroid cancer. J Clin Invest 2005;115:94–101.

10. Pages G, Lenormand P, L'Allemain G, Chambard JC, Meloche S, Pouyssegur J. Mitogen-activated protein kinases p42mapk and p44mapk are required for fibroblast proliferation. Proc Natl Acad Sci U S A 1993;90:8319–23.

11. Welsh CF, Roovers K, Villanueva J, Liu Y, Schwartz MA, Assoian RK. Timing of cyclin D1 expression within G1 phase is controlled by Rho. Nat Cell Biol 2001;3:950–7.

12. Karasarides M, Chiloeches A, Hayward R, et al. B-RAF is a therapeutic target in melanoma. Oncogene 2004;23:6292–8.

13. Hoeflich KP, Gray DC, Eby MT, et al. Oncogenic BRAF is required for tumor growth and maintenance in melanoma models. Cancer Res 2006;66:999–1006.

14. Mitsutake N, Knauf JA, Mitsutake S, Mesa C, Jr., Zhang L, Fagin JA. Conditional BRAFV600E expression induces DNA synthesis, apoptosis, dedifferentiation, and chromosomal instability in thyroid PCCL3 cells. Cancer Res 2005;65:2465–73.

15. Xing M, Westra WH, Tufano RP, et al. BRAF mutation predicts a poorer clinical prognosis for papillary thyroid cancer. J Clin Endocrinol Metab 2005;90:6373–9. Epub 2005 Sep 20.

16. Hingorani SR, Jacobetz MA, Robertson GP, Herlyn M, Tuveson DA. Suppression of BRAF(V599E) in human melanoma abrogates transformation. Cancer Res 2003;63:5198–202.

17. Available from: http://clinicaltrials.gov/show/NCT00405587 and http://www.plexxikon.com/plx-MelanomaColorectal%20Program%20FactSheet_Oct07final.pdf.

18. Ouyang B, Knauf JA, Smith EP, et al. Inhibitors of Raf kinase activity block growth of thyroid cancer cells with RET/PTC or BRAF mutations *in vitro* and *in vivo*. Clin Cancer Res 2006;12:1785–93.

19. Moretti F, Farsetti A, Soddu S, et al. p53 re-expression inhibits proliferation and restores differentiation of human thyroid anaplastic carcinoma cells. Oncogene 1997;14:729–40.

20. Mattiussi S, Turrini P, Testolin L, et al. p21(Waf1/Cip1/Sdi1) mediates shear stress-dependent antiapoptotic function. Cardiovasc Res 2004;61:693–704.

21. Deininger M, Buchdunger E, Druker BJ. The development of imatinib as a therapeutic agent for chronic myeloid leukemia. Blood 2005;105:2640–53.

22. van de Wetering M, Sancho E, Verweij C, et al. The β-catenin/TCF-4 complex imposes a crypt progenitor phenotype on colorectal cancer cells. Cell 2002;111:241–50.

23. van de Wetering M, Oving I, Muncan V, et al. Specific inhibition of gene expression using a stably integrated, inducible small-interfering-RNA vector. EMBO Rep 2003;4:609–15.

24. Smalley KS. A pivotal role for ERK in the oncogenic behaviour of malignant melanoma? Int J Cancer 2003;104:527–32.

25. Knauf JA, Ouyang B, Knudsen ES, Fukasawa K, Babcock G, Fagin JA. Oncogenic RAS induces accelerated transition through G2/M and promotes defects in the G2 DNA damage and mitotic spindle checkpoints. J Biol Chem 2006;281:3800–9.

26. Salvatore G, De Falco V, Salerno P, et al. BRAF is a therapeutic target in aggressive thyroid carcinoma. Clin Cancer Res 2006;12:1623–9.

27. Chiloeches A, Marais R. Is BRAF the Achilles' heel of thyroid cancer? Clin Cancer Res 2006;12:1661–4.

28. Gorospe M, Wang X, Guyton KZ, Holbrook NJ. Protective role of p21(Waf1/Cip1) against prostaglandin A2-mediated apoptosis of human colorectal carcinoma cells. Mol Cell Biol 1996;16:6654–60.

29. Poluha W, Poluha DK, Chang B, et al. The cyclin-dependent kinase inhibitor p21 (WAF1) is required for survival of differentiating neuroblastoma cells. Mol Cell Biol 1996;16:1335–41.

30. Gorospe M, Cirielli C, Wang X, Seth P, Capogrossi MC, Holbrook NJ. p21(Waf1/Cip1) protects against p53-mediated apoptosis of human melanoma cells. Oncogene 1997;14:929–35.

31. Eskandarpour M, Kiaii S, Zhu C, Castro J, Sakko AJ, Hansson J. Suppression of oncogenic NRAS by RNA interference induces apoptosis of human melanoma cells. Int J Cancer 2005;115:65–73.

32. Haapajarvi T, Pitkanen K, Laiho M. Human melanoma cell line UV responses show independency of p53 function. Cell Growth Differ 1999;10:163–71.

33. Fagin JA, Matsuo K, Karmakar A, Chen DL, Tang SH, Koeffler HP. High prevalence of mutations of the p53 gene in poorly differentiated human thyroid carcinomas. J Clin Invest 1993;91:179–84.

34. Ishizaka Y, Ushijima T, Sugimura T, Nagao M. cDNA cloning and characterization of ret activated in a human papillary thyroid carcinoma cell line. Biochem Biophys Res Commun 1990;168:402–8.

35. Gambacorti-Passerini C, le Coutre P, Mologni L, et al. Inhibition of the ABL kinase activity blocks the proliferation of BCR/ABL+ leukemic cells and induces apoptosis. Blood Cells Mol Dis 1997;23:380–94.

AACR American Association for Cancer Research

Molecular Cancer Research

BRAF Silencing by Short Hairpin RNA or Chemical Blockade by PLX4032 Leads to Different Responses in Melanoma and Thyroid Carcinoma Cells

Elisa Sala, Luca Mologni, Silvia Truffa, et al.

Mol Cancer Res 2008;6:751-759. Published OnlineFirst May 5, 2008.